JOURNAL OF MATERIALS SCIENCE 22 (1987) 4307–4312

Laser-induced vapour-phase synthesis of titanium dioxide

J. DAVID CASEY*, JOHN S. HAGGERTY
Massachusetts Institute of Technology, Cambridge, Massachusetts 02139, USA

Small-diameter titanium dioxide powders were synthesized from vapour-phase reactants that were heated with 10.591 μm infrared radiation from a CO_2 laser. Two reactants, titanium isopropoxide and titanium butoxide, were evaluated. Anatase powder was generated from titanium isopropoxide in both static gas and flowing gas configurations. The addition of oxygen to the titanium isopropoxide gas stream reduced the percentage of volatile components in the anatase powder. Detailed characterizations of the product powders are presented.

1. Introduction

The laser-induced vapour-phase synthesis of ceramic powders is a process in which the absorbed infrared radiation from a CO_2 laser provides thermal energy to a reactant gas mixture, inducing the formation of solid products. We have successfully synthesized Si, Si_3N_4, SiC [1–4], B, and TiB_2 [5] powders by this method. Titanium dioxide was the first powder to be synthesized systematically in our laboratory by the laser-induced vapour-phase technique. Others, such as Al_2O_3, have been synthesized in proof-of-concept experiments.

Titanium alkoxides were evaluated as reactants for the TiO_2 synthesis. Advantages of this family of compounds are: the titanium and oxygen atoms are contained within the same reactant molecule, a wide variety of organic groups are available in titanium alkoxide arrangements, some of these organic functional groups have absorption bands in wavelength regions attainable with the CO_2 laser [6–9], and the absorbed laser radiation is expected to initiate controlled decomposition of the organic groups. Disadvantages of titanium alkoxides for the vapour-phase synthesis of TiO_2 are that the alkoxides are liquids at room temperature, a variety of reaction products from the organic groups are possible, and the presence of residual carbon, oxygen and hydrogen in the product powders is anticipated. Titanium isopropoxide, $Ti(i\text{-}OPr)_4$, and titanium butoxide, $Ti(OBu)_4$, are evaluated as reactants in this paper; descriptions of synthesis experiments and powder characterizations follow.

2. Experimental procedure

Descriptions of the flowing gas powder synthesis cell have been published [1, 3, 4], and recent modifications required both to vaporize smoothly liquid reactants and to direct the reactant vapour through the infrared beam of a CO_2 laser beam have also been described [5]. Briefly, a syringe pump is used to meter liquid reactant directly into a heated stainless steel nozzle assembly in which the liquid reactant is quickly vaporized and mixed with other heated reactant gases. This approach was chosen in preference to a bubbler system because thermal decomposition of the titanium alkoxide was possible in the heated bubbler during the course of the experiments and the titanium alkoxide vapour is generated without carrier gas dilution. The hot reactant gas mixture passes up through a vertical 1.4 mm i.d. stainless steel tube into the reaction cell where it is surrounded by a coaxial stream of heated argon gas. The reactant gas stream is intersected by a horizontal CO_2 laser beam, inducing powder formation. The powder is carried by the coaxial argon gas steam into a cylindrical borosilicate-glass resin collection filter (Balston Filter Products, Lexington, Massachusetts) contained in a stainless steel housing unit. The cell pressure is continuously regulated by a solenoid valve positioned on the downstream side of the filter-housing. The downstream side of the solenoid valve is pumped with a rotary oil vacuum pump.

The brightness temperatures of the reaction zone, the volume in which gaseous reactants are converted to hot powders, was measured with an optical pyrometer. To monitor the stability of the reaction process, a photodiode measured fluctuations in a 5 mW HeNe laser beam (λ = 632.8 nm) that passed through the reaction zone. The fraction of the beam transmitted was sensitive to the composition of the reaction zone; fluctuations indicated irregular vaporization of the titanium alkoxide liquid.

Before synthesis reactions were attempted in the flowing gas powder cell, potential reactant gases were evaluated in a static cell (Fig. 1). The static cell is a 10.4 cm long, 2.5 cm i.d. stainless steel cylinder fitted with infrared transparent, KCl windows at both ends. It is equippped with inlet and outlet ports for gases, for a vacuum line, a thermocouple and a manometer. An additional port, sealed with a self-sealing, silicon rubber septum, allows injection of a liquid reactant into the static cell with a syringe while maintaining a leak tight environment in the cell. The cell is positioned within an oven equipped with KCl windows and with holes for the gas lines and diagnostics.

Present address: Avco Speciality Materials, Lowell, Massachusetts 01851, USA.

0022–2461/87 $03.00 + .12 © *1987 Chapman and Hall Ltd.*

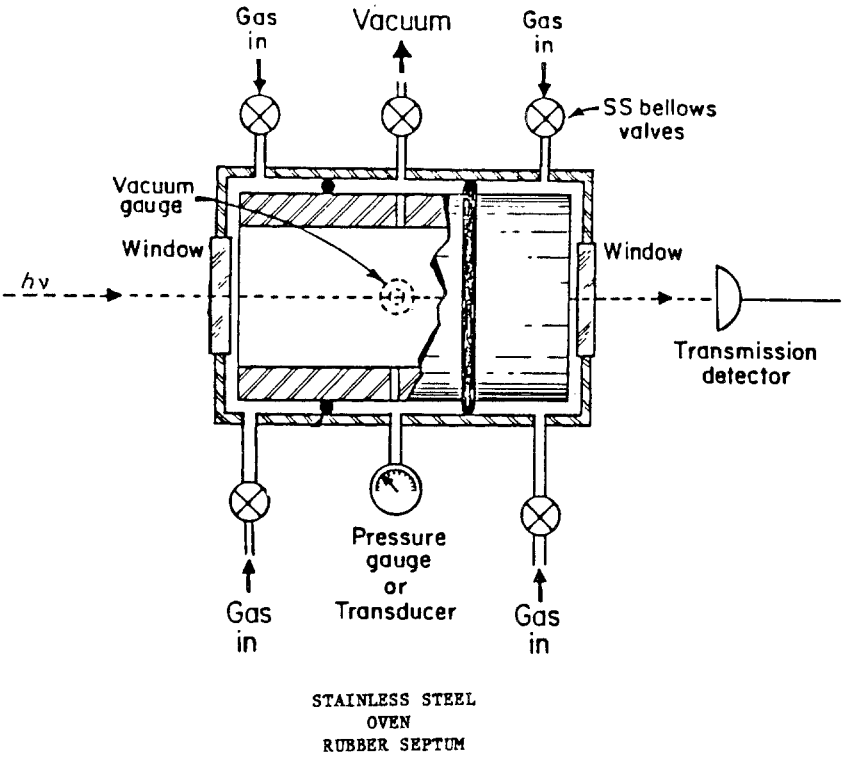

Figure 1 The static cell. See text for details.

Uniform heating of the cell, including its KCl windows, is possible up to approximately 220° C. Importantly, the oven maintains the KCl windows at the same temperature as the stainless steel body of the static cell, thereby preventing condensate from forming preferentially on the cell windows. Pure gases, gas mixtures and vaporized liquids can be subjected to varied laser exposure times and power levels to determine conditions under which powder formation will take place. Powder formation is detected within the cell by observing scattering of a HeNe laser beam passed along the cell axis.

A line-tuneable 50 W CO_2 laser was used for absorptivity measurements and powder syntheses experiments in the static cell. A 150 W, untuned CO_2 laser was used to synthesize powder in the flowing gas powder synthesis cell; this laser provides infrared radiation at a 10.591 μm wavelength, the P(20) line of the (00°1 to 10°0) CO_2 vibrational transition. A 13 cm focal length gallium arsenide lens was used to focus the laser beam.

The titanium isopropoxide and titanium butoxide liquids (Alfa Products, Danvers, Massachusetts) were used without further purification.

The powders were characterized by a number of physical techniques: X-ray diffraction (Cu$K\alpha$), transmission electron microscopy (TEM), single-point BET surface-area analysis, and simultaneous thermal gravimetric and differential thermal analyses (TGA/DTA). Average crystallite sizes were determined from X-ray line width analysis utilizing the Warren and Biscoe line width correction in the Scherer formula [10]. Electron microscopy was done on powder samples prepared by dipping 100 mesh copper TEM grids into ultrasonicated dispersions of the powders in water maintained above pH 10 with a few drops of concentrated ammonium hydroxide. The powders were analysed for titanium, hydrogen, carbon and volatile oxygen (Robertson Laboratory, Inc., Florham Park, New Jersey and Galbraith Laboratories, Knoxville, Tennessee).

3. Results and discussion

3.1. Absorptivity measurements in the static cell

The line-tuneable CO_2 laser was used to investigate absorptivities of gaeous $Ti(i\text{-}OPr)_4$ and $Ti(OBu)_4$ at a number of wavelengths. The first step in the laser-induced vapour-phase process was to determine if sufficient infrared radiation could be absorbed by the candidate reactants to induce a reaction. The literature [6–9] indicated that $Ti(i\text{-}OPr)_4$ has a shoulder in its absorption band at 10.4 to 10.6 μm, within the P branch of the (00°1 to 10°0) CO_2 vibrational emission and that absorption may also occur in the R branch (10.1 to 10.2 μm) of this (00° 1 to 10° 0) emission. The most intense $Ti(i\text{-}OPr)_4$ absorption band is centred at 10 μm; unfortunately the CO_2 laser does not emit at wavelengths within this 10 μm band. The $Ti(OBu)_4$ absorbs in the R (9.2 to 9.3 μm) and P (approximately 9.6 μm) branches of the (00°1 to 02°0) vibrational emission, in the weaker R branch lines (approximately 10.1 and 10.3 μm) of the (00°1 to 10°0) vibrational emission and in the P branch (approximately 11.1 μm) of the (011 to 111) vibrational emission [6, 7].

Absorptivity studies were done at low incident power to minimize gas heating effects. The laser was tuned for maximum powder at a chosen output wavelength; the laser beam was then attenuated to 1 to 2 W with a mechanical chopper (3400 r.p.m.) prior to passing through the static cell. Effective absorptivity values, αP were determined using the relationship

$$\alpha P = \frac{1}{L} \ln\left(\frac{I_0}{I}\right)$$

in which α is the absorptivity ($cm^{-1}\ atm^{-1}$), P is the partial pressure of the absorbing gas (atmosphere), L is the cell path length (10.2 cm), I_0 is the transmitted

TABLE I The αP values for titanium alkoxides at varied CO_2 laser wavelengths

Vibrational transition	Static cell temperature (° C)	Wavelength (μm)	Line designation	αP (cm^{-1}) $Ti(i\text{-}OPr)_4$	αP (cm^{-1}) $Ti(OBu)_4$
(00°1–10°0)	70	10.494	P(10)	0.04	
		10.513	P(12)	0.04	
		10.532	P(14)	0.05	
		10.551	P(16)	0.06	
		10.571	P(18)	0.06	
		10.591	P(20)	0.05	0.02
		10.611	P(22)	0.07	
		10.632	P(24)	0.07	
		10.653	P(26)	0.08	
		10.675	P(28)	0.07	
		10.696	P(30)	0.08	
(00°1–10°0)	60–70	10.195	R(28)		0.07
		10.207	R(26)		0.05
		10.275	R(16)		0.04
		10.319	R(10)		0.05
(00°1–02°0)	150–170	9.250	R(24)		0.21
		9.271	R(20)		0.12
		9.552	P(20)		0.18
		9.586	P(24)		0.20

laser power through the cell in the absence of an absorbing gas and I is the transmitted laser power through the cell containing an absorbing gas. Values of αP were determined at specified cell temperatures for $Ti(i\text{-}OPr)_4$ and $Ti(OBu)_4$ to provide empirical data needed to guide the synthetic procedure, not to determine precisely the absorptivity profiles at various laser wavelengths.

Values of αP for $Ti(i\text{-}OPr)_4$ were determined at a cell temperature of 68 to 70° C, when the vapour pressure is a few torr [11, 12], for the P(10) through P(30) lines of the (00°1 to 10°0) CO_2 transition (Table I); the values ranged from 0.04 cm^{-1} for the P(10) and P(12) lines to 0.08 cm^{-1} for the P(26) and P(30) lines. The αP value was 0.05 cm^{-1} at 10.591 μm, the P(20) line which is generated at relatively high powder levels with untuned CO_2 lasers.

The absorptivity of $Ti(OBu)_4$ was investigated for the R(10) through R(28) lines of the (00°1 to 10°0) vibrational transition (Table I). The αP values ranged from 0.04 cm^{-1} for the R(16) line to 0.07 cm^{-1} for the R(28) line at a cell temperature of 68 to 70° C where the $Ti(OBu)_4$ vapour pressure is approximately 1 torr [11]. The R(34) to R(50) (10.159 to 10.076 μm) and R(4) to R(6) lines (10.365 to 10.350 μm) of the (00°1 to 10°0) transition would overlap better the absorption band of $Ti(OBu)_4$, but we were unable to generate these lines with our line-tuneable laser.

Higher values of αP were determined for $Ti(OBu)_4$ at 150 to 170° C cell temperature for a few lines of the (00°1 to 02°0) transition (Table I), but the vapour pressure of $Ti(OBu)_4$ is still too low (1 to 8 torr) at 150 to 170° C [11] for continuous synthesis of powder at reasonable rates.

Further evaluation of αP at 10.591 μm for $Ti(i\text{-}OPr)_4$ vapour as a function of temperature indicated that a αP increased from 0.05 cm^{-1} at 70° C to 0.5 cm^{-1} at 136° C. This factor suggested that the more volatile $Ti(i\text{-}OPr)_4$ can be used to synthesize powder at 10.591 μm, the wavelength which is available at higher power levels from untuned CO_2 lasers in preference to $Ti(OBu)_4$, which is less volatile and quite transparent at 10.591 μm [7]. Also we anticipated that thermal decomposition of $Ti(OBu)_4$ in the heated nozzle assembly would be a problem because of the elevated temperatures required to generate reasonable vapour mass flow rates into the powder synthesis cell.

3.2. Powder synthesis in the static cell

Following the absorptivity studies, the $Ti(i\text{-}OPr)_4$ vapour was exposed to higher levels of infrared energy from the line tuneable CO_2 laser. Greyish white powder was generated using 10.494 and 10.591 μm wavelengths, the P(10) and P(20) lines of the (00°1 to 10°0) transition. The TiO_2 powders described in this section were synthesized at 10.591 μm. Only small amounts of powder were generated at one time in the heated static cell because powder was deposited throughout the cell, including on the front KCl window. Powder was generated in the static cell from $Ti(i\text{-}OPr)_4$ vapour plus argon, and $Ti(i\text{-}OPr)_4$ vapour plus oxygen; the total cell pressure was approximately 100 torr when argon or oxygen was used. All the powders were greyish white and were generated with an unfocused 10.591 μm laser beam at an intensity of approximately 250 W cm^{-2}.

The properties of powders generated from $Ti(i\text{-}OPr)_4$ in the static cell are summarized in the following paragraphs. Insufficient powder was generated in the static cell to allow detailed comparisons of the effects of argon and oxygen on the powder characteristics.

Characterizations of the powders were done to determine composition, purity, size, shape, and morphology. X-ray diffraction of the powder indicated 20 to 30 nm anatase crystallites [13]. The surface area determined by BET gas desorption was approximately 80 to 90 $m^2 g^{-1}$ with a corresponding 15 to 18 nm equivalent spherical diameter. TGA/DTA in air showed an endothermic weight loss at approximately 80° C and an exothermic phenomenon over a broad temperature region, peaking at 600 to 700° C; the resulting powders were white. Powders heated to

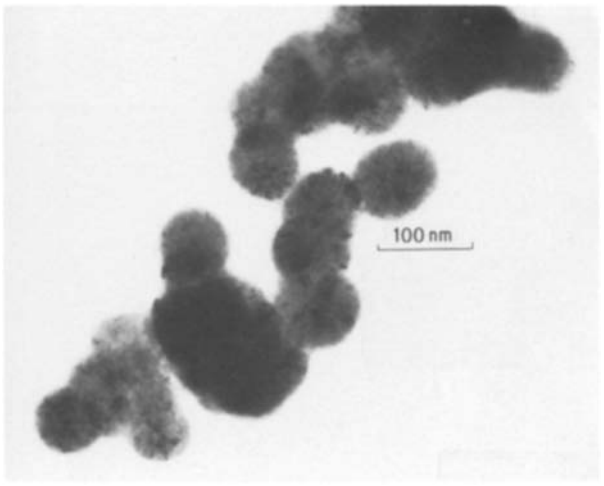

Figure 2 Bright-field transmission electron micrograph of powder generated in the static cell from $Ti(i\text{-}OPr)_4$ vapour.

1200° C under nitrogen were black, an indication of residual carbon in the laser-generated powder. This black coloration was not observed for powders which had been heat treated in air prior to heating in nitrogen. Chemical analyses of the as-synthesized powder indicated 7.7 wt % carbon, 1.2 wt % hydrogen, and 4.5 wt % volatile oxygen. Following heating to 1000 to 1400° C in air, chemical analyses indicated 1 wt % carbon and zero wt % hydrogen and volatile oxygen. The X-ray diffraction pattern of this air-heated powder indicated anatase [13], rutile [14] and possibly Ti_5O_9 [15] phases.

The transmission electron micrographs (TEM) of the as-synthesized powder showed a variety of particle types. Generally, the as-synthesized powders consisted of 60 to 180 nm particles appearing to be clusters of smaller spherical particles (Fig. 2). The difference between BET equivalent spherical diameter and TEM diameters indicates that the as-synthesized particles observed by TEM actually are aggregates of smaller particles with open porosity. After heat treatment in air above 1200° C, the dark-field electron micrographs showed that the particles contained a small fraction of crystallites, approximately 10 nm in diameter. The electron diffraction patterns exhibited some rings consistent with the *d*-spacings of rutile [14]. The particle morphology appeared unchanged by the heat treatment, still consisting of groups of 60 to 180 nm spherical particles.

3.3. Powder synthesis in the flowing gas cell without oxygen gas

The synthesis experiments in the flowing gas powder synthesis cell used a 150 W, 10.591 μm laser beam to heat the $Ti(i\text{-}OPr)_4$ vapour. Representative synthesis conditions and powder characteristics are listed in Table II for reactions with and without oxygen gas.

When the $Ti(i\text{-}OPr)_4$ gas stream, without oxygen addition, was passed through an unfocused (6 mm diameter, 530 W cm^{-2}) beam, a pale orange (700 to 900° C) powder plume was produced. Focusing the beam (1 mm diameter, 2×10^4 W cm^{-2}) produced a bright, white zone where the focused beam and the reaction gas stream intersect; the maximum optical pyrometer brightness temperatures located in this narrow region were 950 to 1300° C. Bright, luminescent, flame-like powder plumes observed during laser-induced thermal breakdown of silane, diborane and boron trichloride have not been observed for the $Ti(i\text{-}OPr)_4$ reaction. The temperature of the heated nozzle assembly, used to vaporize $Ti(i\text{-}OPr)_4$ was kept below 170° C; at approximately 200° C, $Ti(i\text{-}OPr)_4$ decomposition was observed in the nozzle assembly.

The product powders (A-072TO and A-073TO) consisted of beige, grey and white particles, indicating non-uniform composition throughout the powder. The fine powders had fairly large BET surface areas (50 to 70 m^2 g^{-1}) and correspondingly small equivalent spherical diameters (22 to 32 nm). X-ray diffraction indicated the presence of anatase [13] and possibly brookite [16]. X-ray line width analysis indicated 16 to 27 nm anatase crystallites. TGA/DTA in air showed exothermic weight losses at approximately 220, 400 and 500 to 600° C. Weight loss ceased at approximately 600° C. Total weight losses were approximately 17 to 20% for A-072TO powder and 9 to 11% for A-073TO powder which was lighter coloured, suggesting a lower organic content. The pure white powder, formed by heating the A-073TO powder to 600° C in air, had smaller BET surface areas (31 m^2 g^{-1}) and correspondingly larger equivalent spherical diameters

TABLE II Synthesis conditions and powder characteristics of TiO_2 powder

Run number	Laser intensity (10^4 W cm^{-2})	Cell pressure (10^5 Pa)	$Ti(i\text{-}OPr)_4$ sccm*	O_2 sccm*	Brightness reaction zone temperature (° C)	Powder appearance	Surface area† (m^2 g^{-1}) BET	BET equivalent spherical diameter‡ (nm)	X-ray diffraction	Crystallite size§ (nm)
A-072TO	2	0.93–0.98	4.6	0	1300	beige, grey, white	70	22.0	anatase, possibly brookite	16.0–22.0
A-073TO	2	0.66	3.1	0	950–1000	beige, grey, white	49	31.6	anatase	19.0–27.0
A-075TO	2	0.82	2.2–3.0	6	n.d.	light grey	106.7	14.6	anatase	12.6–14.8
A-076TO	2	0.32–0.40	2.2	10–19	800	creamy white	66.6	23.5	anatase	7.5–10.6

*Gas flow units are standard cm^3 min^{-1}.
†Powders were outgassed in BET cell for 2 h at 200° C under nitrogen gas flow before making BET gas desorption measurements.
‡Equivalent spherical diameter for TiO_2 was calculated from BET surface area by using a density value of 3.84 g cm^{-3} for anatase in the equation $d = 6s^{-1}\varrho^{-1}$ in which d is the equivalent spherical diameter, s is the surface area and ϱ is the powder density.
§TiO_2 crystallite size is determined by X-ray line width analysis.
n.d. = not determined.

(50 nm) than the as-synthesized powder. These heated powders exhibited anatase X-ray diffraction patterns [13]. Heating to 1300° C in air produced no further weight changes, but the white TiO_2 powders transformed from anatase to rutile [14] (X-ray). The X-ray line width analysis of the heated powders indicated a 14 to 27 nm crystallite size for both the anatase and rutile phases. Heat treatment of as-synthesized powders in argon to 1400° C produced black powders; X-ray diffraction of these powders showed 13 to 23 nm crystallites of Ti_2O_3 [17].

Electron microscopy of the as-synthesized powder showed groupings of spherical particles; the primary particle size ranged from 15 to 50 nm. Powders heated to 700° C in air appeared as 15 to 50 nm spheres arranged in slightly larger formations than as-synthesized powders. Dark-field microscopy indicated 10 nm anatase crystallites.

3.4. Powder synthesis in the flowing gas cell with oxygen gas

The non-uniform beige, grey and white powder composition produced from $Ti(i\text{-}OPr)_4$ without oxygen and the weight losses which occur during heating in air (9 to 20%) suggested that non-uniform vapour flow through the laser beam and incomplete decomposition of the isopropoxide groups were taking place. We anticipated that the introduction of an oxygen stream into the heated nozzle assembly would facilitate a more even flow of $Ti(i\text{-}OPr)_4$ vapour through the reaction zone and a more complete pyrolysis of the isopropoxide groups. Oxygen addition to a $Ti(i\text{-}OPr)_4$ vapour stream has been shown to cause faster, lower temperature formation of TiO_2 [18].

Table II lists experiments in which oxygen was introduced to the reactant system (A-075TO and A-076TO). Modest $Ti(i\text{-}OPr)_4$ and oxygen mass flow rates were used. A-075TO, which was run at 0.82×10^5 Pa cell pressure, produced a uniformly light grey powder with a BET surface area of 107 $m^2 g^{-1}$ and a correspondingly small equivalent spherical diameter of 14.6 nm. The X-ray diffraction pattern indicated 12.6 to 14.8 nm anatase crystallites. A-076TO powder, produced at lower cell pressure (0.32 to 0.40×10^5 Pa), had a lighter, uniformly creamy white colour. The BET surface area was 67 $m^2 g^{-1}$, corresponding to an equivalent spherical diameter of 23.5 nm. Again, X-ray diffraction of the as-synthesized powder indicated small anatase crystallites (7.5 to 10.6 nm).

During heating in air to 600° C, the greyish A-075TO powder underwent a slightly larger (12 wt %) exothermic weight loss than the creamy white A-076TO sample (5 to 7 wt %). Weight loss began at approximately 100° C and ceased at 450 to 500° C. Continued heating of the powder to 1400° C in air produced no further significant weight loss but did convert the powder from the anatase to the rutile phase.

The chemical analysis of A-075TO and A-076TO powders did not differ greatly. The weight per cent of total volatiles detected by chemical analysis averaged 6 to 10% with 1 to 1.8 wt % carbon, approximately 1 wt % hydrogen and 4 to 8 wt % volatile oxygen. The 600° C heat treatment of these powders in air reduced the total volatiles to 3 to 4 wt %, consisting of 0.3 to 0.5 wt % C, 0.3 to 0.4 wt % H and 2.0 to 3.5 wt % volatile oxygen. After heating to 1400° C in air, only 1 to 2 wt % volatiles remained, the same quantity as detected for a commercial TiO_2 reference standard.

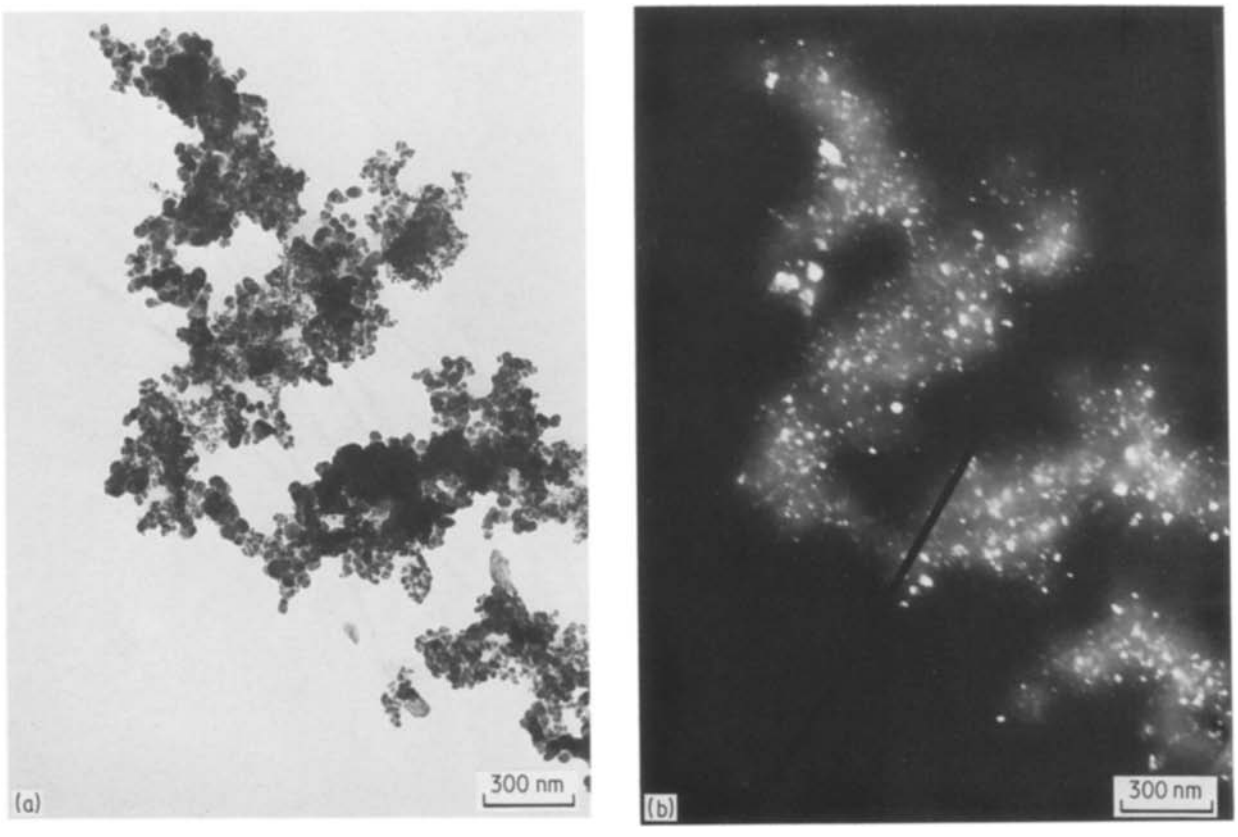

Figure 3 As-synthesized powder generated in the flowing gas cell from $Ti(i\text{-}OPr)_4$ plus oxygen (A-075TO). (a) Bright-field transmission micrograph and (b) the corresponding dark-field micrograph.

After heating the product powders to 600° C in air, the resultant weight of TiO_2 powder correspond to a synthetic yield of 60% for A-075TO and 75% for A-076TO. A factor which reduced the synthetic yield was that some $Ti(i\text{-}OPr)_4$ vapour passed around, rather than through, the focused CO_2 laser beam.

Transmission electron microscopy of both A-075TO and A-076TO powders showed 10 to 70 nm equiaxed particles in large formations (Fig. 3a) which were not successfully dispersed by sonicating in pH 10 to 11 water for 5 to 30 min periods. The corresponding dark-field micrograph (Fig. 3b) shows mostly 10 nm crystallites although some 30 nm particles appear to be single crystals. Both the bright- and dark-field micrographs showed that the 600° C heat treatment in air had minimal effect on the powders.

4. Conclusion

We determined that $Ti(i\text{-}OPr)_4$ was a more viable reactant than $Ti(OBu)_4$ for the laser-induced vapour-phase synthesis of TiO_2 powder. Utilizing an untuned CO_2 laser, fine anatase powders were made from vaporized $Ti(i\text{-}OPr)_4$ with and without oxygen addition. More uniform powders with less volatiles were produced by oxygen addition to the gas stream. Post-synthesis heating in air produced purer anatase powders which converted to rutile at higher temperatures.

Acknowledgements

This work was supported individually by the 3M Company and by a group of industrial sponsors (Abex Corp., Aisin Seiki, Alcoa, Japan Steel Works, NGK Spark Plug, Nippon Steel, Sumitomo Electric and Toa Nenryo Kogyo). Several students and staff, most notably Diana Yoshimura and Kenneth Sinansky, assisted with the research. All contributions are gratefully acknowledged.

References

1. W. R. CANNON, S. C. DANFORTH, J. H. FLINT, J. S. HAGGERTY and R. A. MARRA, *J. Amer. Ceram. Soc.* **65** (7) (1982) 324.
2. W. R. CANNON, S. C. DANFORTH, J. S. HAGGERTY and R. A. MARRA, *ibid.* **65** (7) (1982) 330.
3. J. H. FLINT and J. S. HAGGERTY, "Ceramic Powders from Laser Driven Reactions" SPIE Vol. 458, "Applications of Lasers to Industrial Chemistry" (SPIE – The Industrial Society for Optical Engineering, Bellingham, Washington, 1984) p. 108.
4. Y. SUYAMA, R. M. MARRA, J. S. HAGGERTY and H. K. BOWEN, *Amer. Ceram. Soc. Bull.* **64** (1985) 1356.
5. J. D. CASEY and J. S. HAGGERTY, *J. Mater. Sci.* **22** (1987) 737.
6. V. A. ZEITLER and C. A. BROWN, *J. Phys. Chem.* **61** (1957) 1174.
7. H. KRIEGSMANG and K. LICHT, *Z. Elektrochemie* **62** (1958) 1163.
8. C. G. BARRACLOUGH, D. C. BRADLEY, J. LEWIS and I. M. THOMAS, *J. Chem. Soc.* (1961) 2601.
9. C. T. LYNCH, K. S. MAZDIYASNI, J. S. SMITH and W. J. CRAWFORD, *Anal. Chem.* **36** (1964) 2332.
10. E. W. NUFFIELD, "X-ray Diffraction Methods" (Wiley, New York, 1966) p. 147.
11. R. FELD and P. L. COWE, "The Organic Chemistry of Titanium" (Butterworths, Washington, DC, 1965) p. 36.
12. D. C. BRADLEY, R. C. MEKROTA and W. WARDLOW, *J. Chem. Soc.* (1952) 5020.
13. "X-ray Powder Data File", American Society for Testing and Materials, Philadelphia, Pennsylvania. Data Card 4-0477.
14. *Idem,* Data Cards 4-0551 and 21-1276.
15. *Idem,* Data Card 11-193.
16. *Idem,* Data Card 16-617.
17. *Idem,* Data Card 10-63.
18. M. YOKOZAWA, H. IWASA and I. TERAMOTO, *Jpn J. Appl. Phys.* **7** (1968) 96.

Received 5 January
and accepted 4 March 1987